Green Chemistry

Accepted Manuscript

ROYAL SOCIETY OF CHEMISTRY

www.rsc.org/greenchem

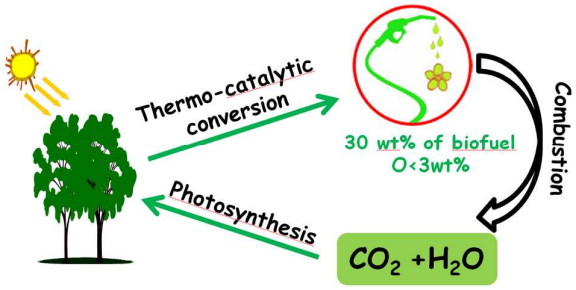

A well dispersed Ru-Cu on HPA catalyst converts pine wood into biofuel (O=3.1 wt%) with a yield up to 30 wt%.

Journal Name

RSCPublishing

ARTICLE

Direct thermo catalytic transformation of pine wood into low oxygenated bio-fuel

Cite this: DOI: 10.1039/x0xx00000x

Walid Al Maksoud,[a,b] Cherif Larabi,[a,b] Anthony Garron,[a,b] Kai C. Szeto,[a] Jean J. Walter[b] and Catherine C. Santini*[a]

Received 00th January 2012,
Accepted 00th January 2012

DOI: 10.1039/x0xx00000x

www.rsc.org/

Direct catalytic conversion of pine wood under H_2 into an organic liquid composed of saturated alkanes and aromatics has been achieved. The resulting organic liquids are easily isolated from the aqueous phase with a yield up to 30 wt%. Importantly, the oxygen content is about 3 wt% and has a Higher Heating Value of 41 MJ/kg which is very close to standard diesel (44MJ/kg) used in automotive fuels. The multi-functional catalysts comprise well size controlled bimetallic nanoparticles (Cu-Ru) supported on heteropolyacid salts. The residual acidic proton of the heteropolyanion salt combined with bimetallic nanoparticle produced a multifunctional catalyst, featuring depolymerisation, deoxygenation and hydrogenation in a single batch reactor. Current results present an alternative approach to transform lignocellulosic biomass (oxygen content higher than 40 wt%) directly to an organic liquid (oxygen content less than 5 wt%) suitable as additives in biofuels.

1. Introduction

The decrease of fossil fuel reserves, primarily crude oil and natural gas, coupled with challenges related to the environment and sustainable restrictions, increase the importance of the use of non-edible biomass feedstocks for generating biofuel and other carbon containing chemicals.[1-2] In European Union, 20% of the conventional fuels used in transportation sector should be replaced by sustainable fuels by 2020. Since the production of bio-fuels should avoid competition with human food feed, it is widely admitted that a sustainable route is the use of lignocellulosic biomass originated from agricultural and wood residues.[3-4] The direct transformation of lignin into organic liquids suitable as additives in conventional fossil fuels has been demonstrated.[5-7] The conversion of lignocellulosic biomass to liquid biofuels (BTL) involves multiple processes, in which depolymerization, decarbonylation and hydrotreatment including hydrocracking, hydrodeoxygenation and hydrogenation are most central steps. Dehydration, depolymerization and decarbonylation,[8-10] as well as hydrocracking reactions,[11] can be achieved by a thermal treatment under inert or reductive atmosphere in the presence of acid catalysts. The dehydroxygenation (HDO) and hydrogenation reactions require transition metal based catalysts.[12-13] The production of biofuel from pine wood requires treatment of biomass at high temperatures under hydrogen with an appropriate catalyst. Moreover, to keep an industrial interest, the energy consumption and the catalysts cost have to be minimized. Recently, we demonstrated that the decomposition of biomass under hydrogen is faster than under argon and occurs at lower temperature.[14]

Under oxidative conditions, heteropolyacid (HPA) are largely used in the transformation of wood into paper pulp,[15] and cellulose into chemicals. More recently, we observed that thermal decomposition temperature of wood is decreased with about 100 °C in the presence of keggin-type heteropolyacid.[16] Due to the low surface area of heteropolyacid, their use in heterogeneous catalysis is carried out by either loading them on supports such as silica[17-18] or replacing some of their protons by large monovalent cations including NH_4^+, Cs^+, Rb^+. In the first approach, HPA dispersion on the surface is ill controlled, because possible reactions with the support causes decomposition or weakness of the HPA structure. In addition, to enable hydrotreatment, further post functionalisation with transition metals are required. However, the distances between the different functionalities of the catalyst are not controlled. The non-soluble cesium exchanged heteropolyanion salt is characterized by high surface area and higher thermal stability. The post modification of the cavities leads to a material with a controlled distances between the acidity of the residual proton and the hydrotreatment active species, thus a well-defined catalyst can in principle be obtained. The acid catalytic activity of heteropolyanion salts in Friedel-Crafts alkylations and dehydration have been described.[19-22] Moreover, the use of bifunctional catalyst for reaction such as Fries rearrangement, lactic acid decarbonylation and deoxygenation of propionic acid have been reported.[23-26] The Ru based catalysts were active in these two reaction in bio-oil valorisation.[27] In addition, the copper-ruthenium based catalysts have been proved to favour the C=O hydrogenation.[28-30] We recently demonstrated that the presence of copper limits the ruthenium nanoparticle growth.[31]

The aim of this work is to combine the depolymerisation ability of Keggin-type heteropolyanion[16] with size controlled ruthenium nanoparticles in order to obtain a multifunctional

catalyst efficient for the direct transformation of pine wood to bio-fuel component. Prior to the catalytic test, the influence of copper on the ruthenium dispersion have been well characterized.

2. Experimental

General procedures

Before the experiments, the pine wood was air-dried, crushed and sieved into powder (<450 µm). Then, the material was dried at 130 °C under continuous flow of argon for 3 h.

$H_3PW_{12}O_4{\cdot}24H_2O$ (Phosphotungstic acid hydrate), Cs_2CO_3 (cesium carbonate), $Cu(NO_3)_2{\cdot}2.5H_2O$ (copper nitrate hemipentahydrate), $RuCl_3$ (ruthenium chloride) (Aldrich) were used as received without further purification.

Preparation of supported mono and bimetallic ruthenium and copper based nanoparticles

The monometallic material based on ruthenium or copper (Ru or Cu) and bimetallic composed of ruthenium and copper (Ru and Cu) catalysts supported on heteropolyacid salts $Cs_{2.5}H_{0.5}PW_{12}O_{40}$ (CsPW) were prepared by wet impregnation according to the literatures.[32]

In a typical reaction, the monometallic ruthenium or copper based catalyst were prepared at room temperature by a dropwise addition of 9.93 ml of an aqueous solution of Cs_2CO_3 (0.2 M) into a mixture of 5.75 g of keggin-type polyoxometalates ($H_3PW_{12}O_{40}{\cdot}24H_2O$) and $RuCl_3$ (0.14 g mg) or $Cu(NO_3)_2{\cdot}2.5H_2O$ (0.277 g). The precipitates obtained were stirred overnight at room temperature. After water evaporation at 50 °C under air, the materials obtained were calcined under dry air at 350 °C for 3 h and reduced under hydrogen at 350 °C during 3 h.

The same procedure was used for the preparation of two samples constituted of bimetallic Ru and Cu with different ratio, supported on CsPW. Typically 5.75 g of $H_3PW_{12}O_{40}{\cdot}24H_2O$ were mixed with $Cu(NO_3)_2{\cdot}2.5H_2O$ and $RuCl_3$ (186 mg, 278 mg and 104 mg, 208 mg respectively) before addition of an aqueous solution of Cs_2CO_3 (9.93 ml, 0.2M) at room temperature, under stirring the water was evaporated. The products obtained were calcined under dry air for 3 h at 350 °C, followed by reduction under hydrogen at 350 °C during 3 h.

Characterization

All the prepared catalysts were characterised by Powder X-ray diffraction (XRD), transmission electron microscopy (TEM), high resolution transmission electron microscopy (HRTEM), elemental analysis (EA), magic angle spinning nuclear magnetic resonance (MAS NMR), N_2 adsorption-desorption and the temperature programmed reduction of oxidised surfaces (s-TPR). The liquids were analysed with gas chromatography–mass spectrometry (GC-MS) and elemental analysis (EA).

Powder X-ray diffraction (XRD) patterns were carried on a Siemens Bruker AXS D-500 instrument using Cu $K\alpha_1$ radiation in bragg-bretano reflecting geometry. Prior to analysis, the sample preparation was done by grinding the material to fine powder, followed by addition of ethanol and in the end deposition of a suspension on a glass plate.

Transmission electron microscopy (TEM) observations were carried out on Philips CM120 instrument with an acceleration voltage up to 120 kV. HRTEM analyses were done with a 200 kV analytical microscope JEM 2100 F from Jeol with an ultrahigh resolution a probe size under 0.5 nm and rapid data acquisition. The HRTEM analyses were supported by energy-dispersive analysis of X-ray spectra (EDAX) to prove the local chemical composition of the nanoparticles observed. The catalysts samples were suspended in toluene and ultrasonically treated for 5 min. Then, a drop of this suspension was disposed uniformly a grid of nickel or molybdenum and dried.

Elemental analyses were performed at the Welience – Pôle Chimie Moléculaire Faculté des Sciences Mirande (Dijon, France), using CHNS/O thermo electron flash 1112 Series elemental analyser (C, H, N) or at the CNRS Central Analysis Department of Solaize (Cs, Cu, Ru, W, P).

Nitrogen adsorption/desorption isotherms of samples were obtained using a volumetric adsorption analyzer (ASAP2020) at −196 ◦C (77 K). Before the adsorption analysis, the samples were degassed for 3 h at 200 ◦C.

^{31}P (121.5 MHz), ^{133}Cs (39.36 MHz) magic angle spinning solid state NMR spectra were collected on a Bruker Avance 300 spectrometer. The impeller zirconia (ZrO_2) of 4 mm was filled with the desired product and sealed with a kel-f stopper, then transferred into the probe Bruker spectrometer allowing rotation of the rotor at a speed of 5 kHz. The time between two acquisitions was always optimized to allow complete relaxation of the nucleus. Chemical shifts were measured relative to 85% H_3PO_4 aqueous solution for ^{31}P and 1M of CsCl for Cs.

The temperature programmed reduction has been performed according to the procedure reported by Bennici et al.[33] using Belcat B device from BEL Japan. H_2 (99.999%) and N_2O (99.990%) were purchased from air liquid. Typically, a sample (200 mg) was first flushed with helium then reduced for 1h at 350 °C using a ramp of 1 °C.min^{-1} under hydrogen (5 Vol% in argon), after that the sample was flushed under argon for 1h and cooled down to 40°C before isothermal oxidation under N_2O (10 vol% in argon). The N_2O was than evacuated under a continuous flowing of argon. Temperature programmed reduction measurement were performed after this treatment under H_2 (5 vol% in argon) for temperatures up to 800°C with a heating rate of 20 °C.min^{-1}.

GC/MS 6850/5975C (Electron energy 70 eV; Emission 300 V; Helium flow rate: 0.7 cm^3/min; Column: HP-5MS (30 m × 0.25 mm × 0.25 µm) was used to analyze the composition of the liquid fractions.

Catalytic evaluation of Ru_xCu_y@CsPW

In the glove box, 10 g of the pine wood powder was mechanically mixed with 1 g of catalyst, the mixture was introduced into a stainless steel batch reactor from Parr instrumentation (capacity: 300 mL, T (max.): 550 °C and P (max.) ~ 140 bar). The batch reactor was connected to a high pressure apparatus and heated under vacuum (10^{-2} mbar) at 70 °C for 30 min under a mechanical stirring (500 rounds/min) in order to remove oxygen and humidity that may be absorbed. Subsequently, 40 bar of hydrogen was introduced in the reactor, before heating to 470 °C (2 °C·min^{-1}). The temperature was maintained at 470 °C for 3 h. Note that the pressure inside the autoclave reached 90-100 bars at 470 °C.

After 3 h at 470 °C, the liquid phase was collected under vacuum to a specific trap placed into liquid nitrogen. The organic phase (bio-oil) was separated from the aqueous by decantation. The water content in the bio-oil was determined by Karl-Fischer method. The organic phase was analysed by GC–MS. The amount of the solid residue left in the reactor consisted mainly of coke and catalysts were weighed.

3. Results and discussion

Keggin-type heteropolyacid are widely used in catalysis due to their higher stability, strong acidity, which is more pronounced than typically strong mineral acids and they are less corrosive, thus their use in stainless steel type reactor is possible. In addition, the exchange of the protons with the monovalent cation leads to the formation of non-soluble salts. The surface area increases with the cesium content. In this work, cesium carbonate was chosen as a source of cesium cation. The reaction of the cesium carbonate with keggin-type heteropolayacid gives corresponding salts, water and carbon dioxide, purification of the solid are avoided. Phosphotungstic acid ($H_3PW_{12}O_{40}$) is described to have higher stability and acidity compared to corresponding silicon or molybdenum based heteropolyacid. 2.5 over 3 equivalent of the proton were replaced by cesium atom ($Cs_{2.5}H_{0.5}PW_{12}O_{40}$), in order to keep residual protons to favour the pyrolysis under acid condition. Furthermore, a high surface area is obtained, which allow its use as support for ruthenium and copper nanoparticles to enable the hydrotreatment. The most characteristic data of the catalysts referred to Ru@CsPW, Cu@CsPW and RuCu@CsPW.

3.1. Characterization of the catalysts

Textural properties of the different catalysts were examined by nitrogen adsorption-desorption isotherm measurements, the obtained surfaces area are summarized in Table 1.

Table. 1: Surface area and elemental analysis of the catalysts

Catalysts	*Surface BET ($m^2.g$-1)b*	*Ru/Cu content expected (Wt%)c*	*Ru/Cu content measured (Wt%)*
CsWP	150	0/0	0/0
Cu@CsWP	120	0/1	0/1.1
Ru@CsWP	89	1/0	1.3/0
Ru_1Cu_1@CsWP	68	1/1	0.8 / 1.1
Ru_2Cu_1@CsWP	60	2/2	1.9 / 1.4

The shape of these material isotherms, as shown in Fig. 1, corresponds to type IV according to IUPAC classification and display H3 type hysteresis loop characteristic of capillary condensation between the aggregates composing the solid. The initial increase in adsorption capacity at low relative pressure is due to monolayer adsorption. The upward deviation in the range of $P/P_0 = 0.7$-0.9 for the support and the monometallic catalyst is associated with progressive filling of the space between the aggregates of particles composing the support. The neat support $C_{2.5}H_{0.5}PW_{12}O_{40}$ has specific surface area *ca.* 150 $m^2.g^{-1}$ as already reported in the literature.[22-23] The isotherms of the bimetallic catalyst reach a plateau for the pressures $P/P_0 >$ 0.5. The hysteresis loop as well as the surface area decrease with the loading of the metal nanoparticles. As expected, the post modification of the support by introducing metal complexes lowers the surface area to *ca.* 120 and 88 $m^2.g^{-1}$ for catalyst loaded with 1 wt% of copper and 1.3 wt% of ruthenium respectively. The surface area of the bimetallic catalysts are about 68 for the catalyst comprising 0.8 wt% of ruthenium and 1.1 wt% of copper, and it is solely 60 $m^2.g^{-1}$ for the catalyst containing 1.4 and 1.9 wt% of the copper and ruthenium respectively. This indicates that the pores of the solids are partially filled with the metal catalyst.

The amounts of the metals (ruthenium and copper) present in different prepared catalysts are measured by ICP. As shown in Table 1, the experimental results are close to the expected values, the little discrepancies can be explained by the amount of water adsorbed on different starting compounds since the given moisture content in each product was considered in the calculation.

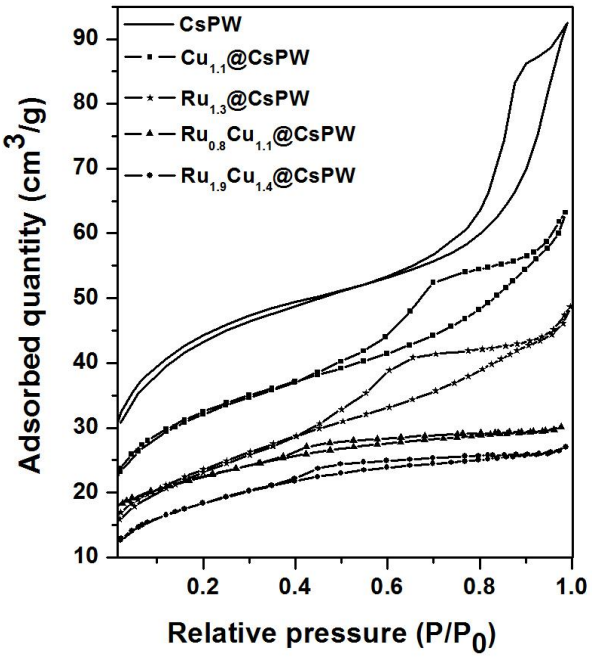

Fig. 1 Nitrogen adsorption/desorption isotherms of different samples

Elemental analysis of the CsPW sample targeted to $Cs_{2.5}H_{0.5}PW_{12}O_{40,}$ revealed the Cs, H, P, W contents are 10.09, 0.61, 0.92, 64.85 wt% respectively (estimated amount of oxygen is 24 wt%). These results describe a compound with a molecular formula $Cs_5HP_2W_{23}O_{80}{\cdot}20H_2O$ (or $Cs_{2.5}H_{0.5}PW_{11.5}O_{40}.10H_2O$) which is close to the expected formula.

The powder XRD analyses of monometallic and bimetallic catalysts as well as the support in the range of 4-70° of 2Θ are provided in Fig.S1. In general, the reported diffractograms are very similar to the one collected for the cesium exchange heteropolyanion. The diffraction pattern of CsPW shows only one phase close to the cubic structure of $H_3PW_{12}O_{40}$.[34] No shifting or additional reflections induced by the copper or ruthenium nanoparticles deposited on the support are observed, indicating that the crystalline structure of the support is preserved with the metal loading and during the thermal treatment under oxygen and hydrogen. Moreover, absence of diffraction peaks from the metals can be explained by the low metal loading or the nanoparticles are well dispersed and too small for all samples.

The ^{31}P, ^{133}Cs MAS NMR spectra of the support CsPW and the other catalyst are displayed in Fig.S2. ^{31}P spectra are characterized by two peaks at -15 ppm and -13 ppm assigned to crystalline polyanionic species. The presence of two peaks is attributed to the dehydration of the heteropolyanion as already observed.[35] ^{133}Cs MAS NMR spectra of Cs^+ cations introduced into the heteropolyanion lattices are presented in Fig.S2, and show only one peak at -51 ppm flanked with spinning sidebands. When the sample is exposed to moisture, the peak is downshifted and appeared at -56 ppm (Fig.S3) as reported in literature,[22] as it is well described that the ^{133}Cs NMR is very sensitive to water.[34]

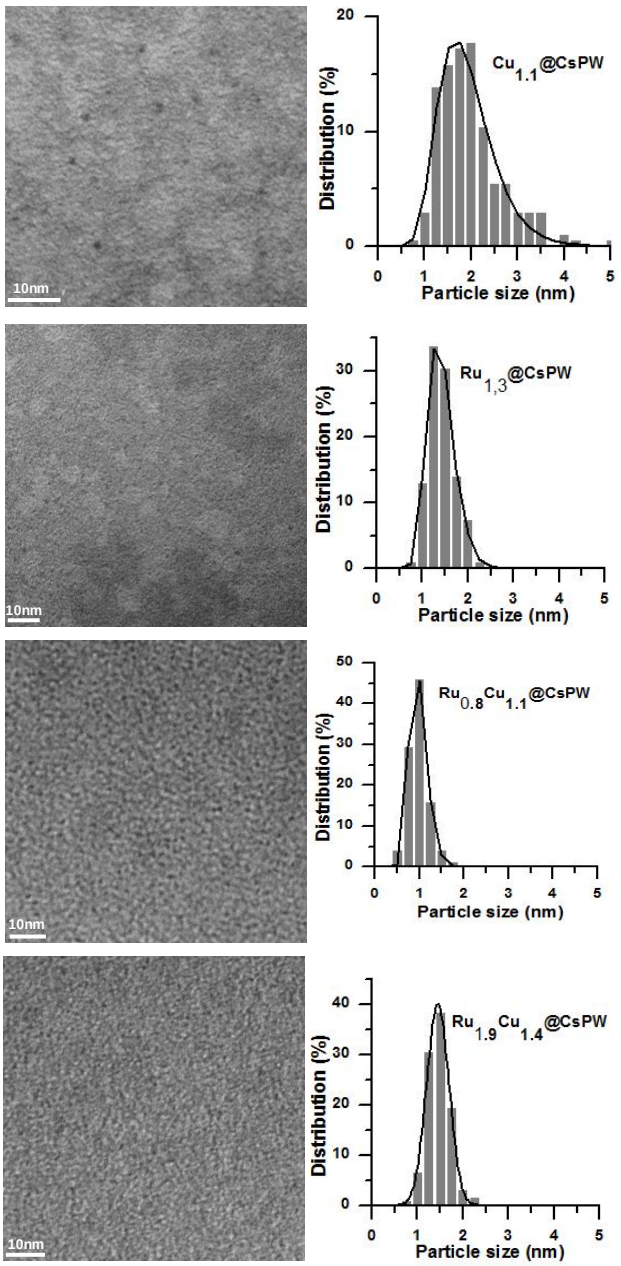

Fig. 2 TEM micrographs of the catalysts $Cu_{1.1}$@CsPW, $Ru_{1.3}$@CsPW, $Ru_{0.8}Cu_{1.1}$@CsPW and $Ru_{1.8}Cu_{1.4}$@CsPW from top to down respectively.

Fig. 2 shows typical TEM images of Cu, Ru and RuCu supported on CsPW catalyst. The metal nanoparticles are highly dispersed for all catalyst. Ru based catalyst presented a narrow distribution of particles (± 0.3 nm), while Cu catalyst has a broad size distribution (2-3 nm). In addition, the bimetallic catalysts comprises small particles, with a means size of 0.9±0.2 nm and 1.3±0.3 nm for $Ru_{0.8}Cu_{1.1}$@CsWP and $Ru_{1.9}Cu_{1.4}$@CsWP respectively. The size of the combined bimetallic nanoparticles is smaller compared to the corresponding monometallic catalyst. These highly dispersed nano-sized metallic particles have been observed when the loading in Ru is increasing for a constant amount of Cu.[31]

In order to further reveal the detailed structure of the supported bimetallic samples, HRTEM and EDX are performed. Fig.S4 shows typical HRTEM images on the samples and the corresponding FFT estimation of the lattice parameters. Their comparison leads to the observation of metal oxides (monoclinic CuO, tetragonal RuO_2 and cubic RuO_4). However, when the analyses are performed under hydrogen atmosphere, hexagonal Ru(0) nanoparticle are present (Fig.S4 micrograph a)). The particles are very small and quit unstable under electron beam, making difficult to perform EDX analysis of the particle. Nevertheless, the local EDX analyses (Fig.S5) indicated the presence of ruthenium and copper very close to each other.

The redox properties of the catalysts were studied by temperature programmed reduction techniques of oxidized surfaces (s-TPR). S-TPR profiles of the samples are highlighted in Fig.3. The heteropolyanion support showed H_2 consumption in the temperature range 550-800 °C attributed to the reduction of the tungsten oxide of the support. Contrary to Cu/Al_2O_3 catalyst, where the copper is reduced at 300 °C (Fig. S6), Cu@CsWP showed only low H_2 consumption at 300 and 500 °C. A large H_2 uptake is observed at temperature higher than 700 °C due to the reduction of the support (Fig. 3a). This result could be attributed to both a strong interaction between Cu and the support (CsPW) and the hindering of Cu.

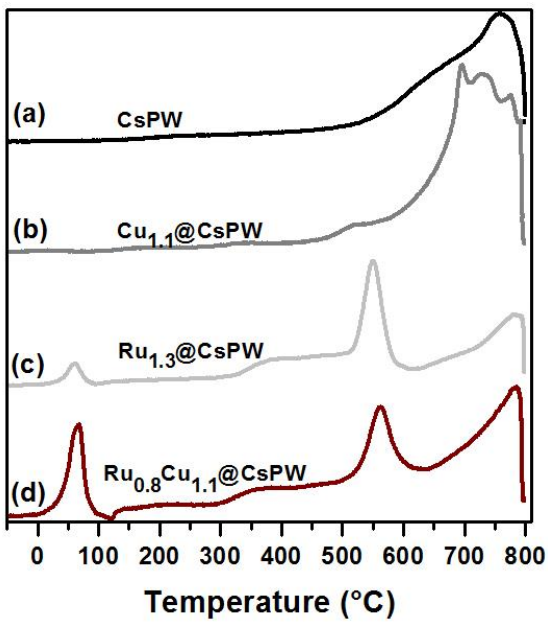

Fig. 3 s-TPR profiles of the support CsPW (a), as well as the catalysts $Cu_{1.1}$@CsPW (b), $Ru_{1.3}$@CsPW (c) and $Ru_{0.8}Cu_{1.1}$@CsPW (d).

Two main H_2 uptakes are observed for the ruthenium based catalysts at 70 and 550 °C(Fig .3c), ascribed to metallic Ru and RuO_x respectively. As for Cu@CsPW catalyst, the s-TPR profiles of $Ru@Al_2O_3$ is different from the one observed for Ru@CsWP (Fig. S7) highlighting again a strong effect of CsPW support.[36]

The amount of hydrogen adsorbed at 70 °C increases when the Ru based catalyst is doped with copper which is in agreement with TEM data showed the formation of smaller size Ru-Cu particles. The H_2 consumption increases from 33 to 56 $\mu mol.g^{-1}$ which can correspond to an increase of the Ru dispersion. The Cu presence allows a redistribution of the Ru metallic phase and can also play a role on the catalyst hydrogenation ability by spill-over between Ru and Cu as demonstrated by King et al.[37]

3.2. Comparison of catalytic performances

The conversion of the biomass (10 g of pine wood) in the presence of 10 wt% of the catalysts described before (*vide supra*) and the support solely (CsPW), as well as the blank have been performed in a batch reactor at 470 °C under 40 bars of hydrogen for 3h. Five main fractions were recovered: gas, aqueous, organic, acetone soluble residue (polymer), non-soluble residue (coke). The collected fractions were weighed, while the gas phase was estimated, the obtained results are summarized in Table 2

Table. 2 yield of different fractions obtained during the catalytic hydro-treatment of pine wood.

Catalysts	*Aqueous liquid*	*Organic liquid*	*Gas*	*Coke*	*Polymer*
1.Blank	*30*	*3*	*22*	*42*	*3*
2.CsPW	*30*	*7*	*21*	*38*	*3*
3.$Cu_{1.1}$@CsPW	*32*	*10*	*18*	*35*	*5*
4.$Ru_{1.3}$@CsPW	*40*	*25*	*23*	*7*	*5*
5.$Ru_{0.8}Cu_{1.1}$@CsPW	*39*	*21*	*20*	*13*	*7*
6.$Ru_{1.9}Cu_{1.4}$@CsPW	*36*	*29*	*17*	*11*	*7*

In all experimental tests, the amount of the gas phase is around 20 wt% and composes mainly of CO, CO_2, light alkanes (C_nH_{2n+2}). Their proportion are reported elsewhere.[14,16]

In the absence of catalyst (blank), run 1, a low conversion is observed, 33 wt% liquid (mainly aqueous phase 30 wt% and 3 wt% of organic phase) and 42 wt% of a residual solid charcoal is left. The support (CsWP), run 2 exhibits similar activity, liquid phase is slightly increased to 37 wt% (30 wt% of aqueous phase and 7 wt% of organic phase) and the residual solid constituted 38 wt%. The biomass treatment in the presence of copper based catalyst ($Cu_{1.1}$@CsWP), run 3 leads to minor increasing of organic phase (10 wt%).

More than 65 wt% of the wood was converted into liquids, in the presence of ruthenium based materials, runs (4, 5, 6). The amount of organic phase is seven to ten times higher than in runs (1-3), the quantity of the residual solid, mostly composed of coke is only 10 wt%. The organic phases contain less than 1 wt% of water measured by mean of Karl-Fischer method. A maximum yield in organic phase is obtained with $Ru_{1.9}Cu_{1.4}$@CsPW catalyst (run 6), where it was around 29 wt%.

The amount of oxygen is a crucial factor in biofuels application, thus the elemental content of C, H, O of the organic fractions are measured. The composition of organic and soluble solid (polymer) phases as well as the amount of carbon still present in then aqueous fraction obtained for the catalytic tests (run 4, 5 and 6) are summarized in Table 3.

Table. 3 Weight composition of the liquid phases for the ruthenium-based catalysts determined by elemental analyzer

Catalysts	*Organic phase C/H/**O**^{a}(wt%)*	*Carbon in aqeous phase (wt%)*	*Polymer phase C/H/**O**^{a} wt%)*
4.$Ru_{1.3}$@CsPW	79.0/13.0/**7.2**	4	83.8/9.4/**6.5**
5.$Ru_{0.8}Cu_{1.1}$@CsPW	84.0/11.5/**4.1**	2.2	nd
6.$Ru_{1.9}Cu_{1.4}$@CsPW	84.6/12.0/**3.1**	2	82.6/8.4/**8.2**

These results show that the organic phase contained 3.1 wt% of oxygen when the wood was treated with $Ru_{1.9}Cu_{1.4}$@CsPW catalyst (run 6), 4.1 wt% with $Ru_{0.8}Cu_{1.1}$@CsPW (run 5) and 7.2 wt% with $Ru_{1.3}$@CsPW (run 4). The oxygen content decreased with the increasing of the amount of ruthenium in the catalyst. The GC-MS analyses indicate that more hydrogenated compounds are obtained also with the catalyst contain higher amount of ruthenium as reported in the literature.[8] The combination of the copper with ruthenium leads to a formation of organics with low oxygen content (7.2, and 4.1 wt% in run 4 without copper and run 5 with 1.1 wt% of copper respectively), In addition, the amount of carbon measured in aqueous phases is low for samples treated with bimetallic based catalyst (around 2 wt%) suggesting that Ru-Cu based catalyst convert oxygenated chemicals to non-polar products, thus are more active in hydrogenation and hydrodeoxygenation.[29] The polymeric phases (yield 7 wt%) formed through the coupling reaction between the furan moieties[38] contained around 83 wt%, of carbon and 8.5 wt% of hydrogen.

In order to determine the effect of the catalysts on the reaction, three isolated organic phases from runs (4-6) have been analyzed by GC-MS, Fig.4 and Table 4.

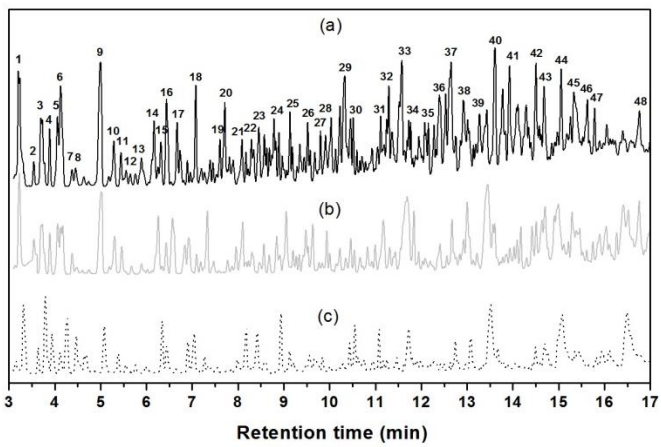

Fig. 4 Chromatograms of the organic phases recovered after the pine wood treatment under hydrogen in presence of $Ru_{1.9}Cu_{1.4}$@CsPW (a), $Ru_{0.8}Cu_{1.1}$@CsPW (b) and $Ru_{1.3}$@CsPW (c).

Table 4: The chemicals products attributed to numbers represented in different GC MS chromatograms

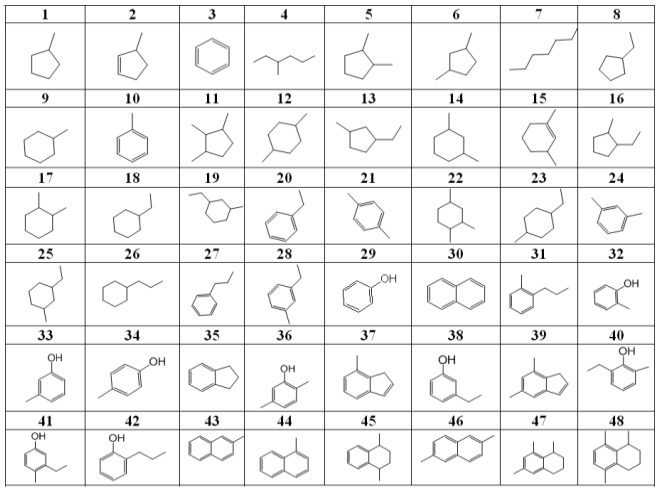

With Ru@CsPW, besides some aromatics (3, 24, 31, 44) and fully hydrogenated aromatic (9, 18) the most intense peaks were identified as phenol derivatives (29, 31, 34 38, 40-42, 50, 51).

With bimetallic catalysts, more chemicals are obtained and increases with the Ru loading. Concomitantly, the intensities of the peaks assigned to phenol derivatives decrease (e.g. 34) and some disappeared (e.g. 50, 51), thereby decreasing the oxygen content (runs 5, 6). The resulting organic phase presents a measured Higher Heating Value of 41 MJ.kg^{-1} close to the one of standard diesel (44 MJ.kg^{-1}).

Concerning the yield in the various product phases, the amount is similar to both the bimetallic and monometallic ruthenium catalysts. The catalytic activity of the bimetallic samples is driven by the ruthenium phase and not by copper (run 3). This predominance of the fully hydrogenated organics demonstrated the high hydrogenation ability of the Ru NPs. In the presence of copper the HDO reaction, crucial reaction for the fuel production is favoured.[39] The copper is not an efficient metallic phase for hydrogenation reaction compared to conventional hydrotreating metal (Ni, Co, Ru, Pt, Pd,…),[13] however Cu and especially CuO are known for their redox properties and their effect on the size and shape control of the resulting bimetallic catalysts.[40] In Ru_xCu_y@CsPW catalysts, Cu induces the formation of small particle size (TEM and s-TPR) inducing a higher catalytic activity in hydrogenation (Fig. 4a vs Fig. 4c) as well as in the HDO reaction (oxygen content decreases from 7.2 to 3.1 wt% see Table. 3) .

3.3. Recycling

Efforts to recycle the catalyst by recovering the insoluble solid after the test were made. In fact, the recycling directly from the residual solid as well as from the washed residual solid has been tested. In both cases, no specific catalytic activity has been observed due to the non-accessibility of the metal buried into the coke. The recycling procedure consists on first burning deposited carbon under continuous flow of oxygen at 450 °C for 6 h, followed by washing with water acidified to 5 % with acetic acid (in order to remove the mineral salt coming from wood dust) and then drying of the resulting powder. Then the obtained solid was reduced at 350 °C under hydrogen flow for 3h in order to recover the metallic state of ruthenium. The catalyst recycled was tested under the same conditions. Four cycles are performed with the same catalyst and the yields of organic fraction are highlighted in Fig.5.

Fig. 5 Yield of organic phase obtained with the four times recycled

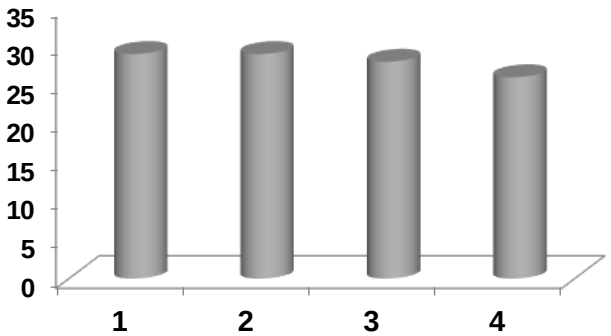

$Ru_{1.9}Cu_{1.4}$@CsPW catalyst.

The yield of organic is slightly decreased from 29 to 26 wt%, simultaneously, the amount of oxygen increased with about 1.5 wt% for each cycle, from 3.1 wt% for the first cycle to 7.8 wt% for the fourth cycle. TEM performed on this catalyst (Fig.S6) showed that the metallic nanoparticles have a tendency to grow with the different thermal treatment under hydrogen and oxygen. The oxygen content of organic phase can be decreased by increasing the reaction time (more than 3h).

4. Conclusion

The bimetallic Ru and Cu based catalysts (Ru_xCu_y@CsPW) supported on heteropolyanion are synthesized by wet impregnation of the ruthenium and/or copper precursors on a strong acidic support $Cs_{2.5}H_{0.5}PW_{12}O_{40}$ (CsPW). A synergetic effect inducing the formation of smaller bimetallic nanoparticles compared to single metals is observed. These highly dispersed nano-sized bimetallic particles exhibit a high homogeneity and a particle size depending on the Ru content when the amount of Cu remains constant.

The catalytic activity of a multifunctional catalyst in conversion of pine wood under hydrogen into biofuel has been evaluated in batch reactor. 30 wt% of organic liquid are isolated in the presence of catalyst while only traces are obtained without catalyst. The GC-MS analyses indicated that the organic phase is composed of saturated alkanes and aromatics constituted of 3.1 wt% of oxygen. The HHV of the organic phase is found to be 41 MJ.kg^{-1} (Diesel = 44 MJ.kg^{-1}). This work demonstrated the possible one step catalytic conversion of biomass into biofuel. Improvement in the stability of the catalyst can be carried out by either introducing third metal such as nickel to enable hydrogenation and lowering the price of catalyst, or by dispersing this catalyst on a support with high surface area including SBA-15, MCM-41. This catalytic system can be used also to convert lignin which is side product of pulp mill industry into fuel.

Acknowledgements

Thanks to Dr. P. ARQULLIERE (C2P2, IR) for performing the TEM analyses.

Notes and references

[a] Université de Lyon, ICL, C2P2, UMR 5265 CNRS-ESCPE Lyon, 43 bd du 11 Novembre 1918, 69616 Villeurbanne Cedex, France.
E-mail: catherine.santini@univ-lyon1.fr
[b] Synthopetrol, 37 Rue des Maruthins 75008 Paris 8, France.

1 G. W. Huber, S. Iborra and A. Corma, *Chem. Rev.*, 2006, **106**, 4044.
2. D. M. Alonso, J. Q. Bond and J. A. Dumesic, *Green Chem.*, 2010, **12**, 1493.
3. J. C. Serrano-Ruiz, R. Luque and A. Sepulveda-Escribano, *Chem. Soc. Rev.*, 2011, **40**, 5266.
4. M. Stöcker, *Angew. Chem., Int. Ed.*, 2008, **47**, 9200.
5. M. J. Climent, A. Corma and S.Iborra, *Green Chem.*, 2014, DOI: 10.1039/c3gc41492b/
6. Q. Bu, H. Lei, A. H. Zacher, L. Wang, S. Ren, J. Liang, Y. Wei, Y. Liu, J. Tang, Q. Zhang and R. Ruan, *Bioresour. Technol.*, 2012, **124**, 470.
7. M. Kleinert and T. Barth, *Energy & Fuels*, 2008, **22**, 1371-1379.
8. J. N. Chheda and J. A. Dumesic, Catal. Today, 2007, **123**, 59-70.
9. A. K. Agarwal, *Prog. Energy Combust. Sci.*, 2007, **33**, 233-271.
10. Y. Wan, P. Chen, B. Zhang, C. Yang, Y. Liu, X. Lin and R. Ruan, *J. Anal. Appl. Pyrol.*, 2009, **86**, 161.
11. A. Corma, G. W. Huber, L. Sauvanaud and P. O'Connor, *J. Catal.*, 2007, **247**, 307.
12. P. M. Mortensen, J. D. Grunwaldt, P. A. Jensen, K. G. Knudsen and A. D. Jensen, *Appl. Catal. A*, 2011, **407**, 1.

13. E. F. Iliopoulou, S. D. Stefanidis, K. G. Kalogiannis, A. Delimitis, A. A. Lappas and K. S. Triantafyllidis, *Appl. Catal. B*, 2012, **127**, 281.
14. C. Larabi, W. Al Maksoud, K. C. Szeto, O. Boyron, A. Roubaud, P. Castelli, C. C. Santini and J. J. Walter, *J. Anal. Appl. Pyrol.*, 2013, **100**, 81.
15. A. R. Gaspar, J. A. F. Gamelas, D. V. Evtuguin and C. P. Neto, Green Chem., 2007, 9, 717-730.
16. C. Larabi, W. Al Maksoud, K. C. Szeto, A. Roubaud, P. Castelli, C. C. Santini and J. J. Walter, *Bioresour. Technol.*, 2013, **148**, 255.
17. V. Dufaud, F. Lefebvre, G. P. Niccolai and M. Aouine, *J. Mat. Chem.*, 2009, **19**, 1142.
18. P. Putaj and F. Lefebvre, *Coord. Chem. Rev.*, 2011, **255**, 1642.
19. N. Essayem, G. l. Coudurier, J. C. Vedrine, D. Habermacher and J. Sommer, *J. Catal.*, 1999, **183**, 292.
20. N. Essayem, A. Holmqvist, P. Y. Gayraud, J. C. Vedrine and Y. Ben Taarit, *J. Catal.*, 2001, **197**, 273.
21. W. Deng, Q. Zhang and Y. Wang, *Dalton Trans.*, 2012, **41**, 9817.
22. A. Molnar, T. Beregszaszi, Ã. Fudala, P. Lentz, J. B. Nagy, Z. Kanya and I. Kiricsi, *J. Catal.*, 2001, **202**, 379.
23. E. F. Kozhevnikova, E. Rafiee and I. V. Kozhevnikov, *Appl. Catal. A*, 2004, **260**, 25.
24. I. V. Kozhevnikov, *J. Mol. Catal. A*, 2009, **305**, 104.
25. B. Katryniok, S. Paul and F. Dumeignil, *Green Chem.*, 2010, **12**, 1910.
26. H. W. Park, S. Park, D. R. Park, J. H. Choi and I. K. Song, *Catal. Commun.*, 2010, **12**, 1.
27. D. C. Elliott and T. R. Hart, *Energy & Fuels*, 2009, **23**, 631.
28. D. S. Shephard, T. Maschmeyer, G. Sankar, J. M. Thomas, D. Ozkaya, B. F. G. Johnson, R. Raja, R. D. Oldroyd and R. G. Bell, *Chem. Eur. J.*, 1998, **4**, 1214-1224.
29. J. Alvarez-Rodriguez, B. Bachiller-Baeza, A. Guerrero-Ruiz, I. Rodriguez-Ramos and A. Arcoya-Martin, *Catal. Today*, 2008, **133**, 793-799.
30. N. Atamena, D. Ciuculescu, G. Alcaraz, A. Smekhova, F. Wilhelm, A. Rogalev, B. Chaudret, P. Lecante, R. E. Benfield and C. Amiens, Chem. Commun., 2010, **46**, 2453-2455.
31. P. Arquilliere, P-H. Haumesser, I. Helgadottir, C. C. Santini, M. Aouine, L. Massin and J-L. Rousset, *Top. Catal.*, 2013, **56**, 1192.
32. J.-J. Walter, C. Santini-Scampucci, C. Larabi and W. Al Maksoud, *WO 2013128120*, 2013, 81pp.
33. A. Gervasini and S. Bennici, *Appl.Catal. A*, 2005, **281**, 199-205.
34. T. Okuhara, H. Watanabe, T. Nishimura, K. Inumaru and M. Misono, *Chem. Mat.*, 2000, **12**, 2230.
35. X. Xu, A. G. Kalinichev and R. J. Kirkpatrick, *Geochimica et Cosmochimica Acta*, 2006, **70**, 4319.
35. B. M. Faroldi, J. F. Munera and L. M. Cornaglia, *Appl. Catal. B.*, 2014, **150-151**, 126.
37. M. W. Smale and T. S. King, *J. Catal.*, 1989, **119**, 441.
38. C. Méalares, Z. Hui and A. Gandini, *Polymer*, 1996, **37**, 2273.
39. M. Badawi, J. F. Paul, S. Cristol, E. Payen, Y. Romero, F. Richard, S. Brunet, D. Lambert, X. Portier, A. Popov, E. Kondratieva, J. M. Goupil, J. El Fallah, J. P. Gilson, L. Mariey, A. Travert and F. Mauge, *J. Catal.*, 2012, **282**, 155-164.
40. A. M. Karim, V. Prasad, G. Mpourmpakis, W. W. Lonergan, A. I. Frenkel, J. G. Chen and D. G. Vlachos, *J. Amer. Chem. Soc.*, 2009, **131**, 12230.